processes

MDPI

Article

Novel Anthracene HTM Containing TIPs for Perovskite Solar Cells

Sanghyun Paek

Department of Chemistry and Energy Engineering, Sangmyung University, Seoul 03016, Korea; sanghyun.paek@smu.ac.kr

Abstract: Recently, perovskite solar cells have been in the spotlight due to several of their advantages. Among the components of PSCs, hole transporting materials (HTMs) re the most important factors for achieving high performance and a stable device. Here, we introduce a new D–π–D type hole transporting material incorporating Tips-anthracene as a π–conjugation part and dimethoxy-triphenylamine as a donor part (which can be easily synthesized using commercially available materials). Through the measurement of various optical properties, the new HTM not only has an appropriate energy level but also has excellent hole transport capability. The device with **PEH-16** has a photovoltaic conversion efficiency of 17.1% under standard one sun illumination with negligible hysteresis, which can be compared to a device using Spiro_OMeTAD under the same conditions. Ambient stability for 1200 h shown that 98% of PEH-16 device from the initial PCE was retained, indicating that the devices had good long-term stability.

Keywords: perovskite solar cells; hole transporting materials; stability; anthracene derivatives

Citation: Paek, S. Novel Anthracene HTM Containing TIPs for Perovskite Solar Cells. *Processes* **2021**, *9*, 2249. https://doi.org/10.3390/pr9122249

Academic Editor: Ioannis Spanopoulos

Received: 3 November 2021
Accepted: 13 December 2021
Published: 14 December 2021

1. Introduction

Perovskites of organic–inorganic hybrid halide have become one of the most promising next-generation photovoltaic materials due to their unique properties such as their large charge-carrier diffusion length [1], small exciton binding energy [2], high absorption coefficient [3], and low trap density [4], all of which have pushed their performances to a record efficiency beyond 25.5% [5]. Hole transporting materials (HTMs) are one of the most important factors for achieving high performance in perovskite solar cells (PSCs). HTMs exhibit an important role in PSCs to transfer the positive charges in between perovskite and counter electrodes [6–10]. Among the various HTMs, 2,2′,7,7′-tetrakis(*N*,*N*-di-p-methoxyphenylamine)-9,9′-spirobifluorene (Spiro_OMeTAD) has been widely used in PSCs. However, it is necessary to develop new HTMs to replace their low stability and good price in future application of PSCs.

Many researchers have widely used dimethoxy-arylamine as a donor part due to its superior hole transporting ability. Moreover, researchers have developed arylamine (Donor)–spacer (π-conjugation)–arylamine (Donor) materials that can synthesize new HTMs through simple changes. Donor-π-Donor configured HTMs such as thiophene derivatives [11,12], carbazole derivatives [13,14], and fluorene-dithiophene [15] flanked by amine donors are widely studied in PSCs to replace their expensive price and instable spiro-OMeTAD. Among them, anthracene-base molecules have potential properties and are well known for applications such as organic solar cells, light-emitting diodes, organic thin film transistors, and perovskite solar cells [16–20]. Recently, X. Liu reported a PEC of 17.27% using anthracene HTMs by simple synthesized [21]. Particularly, A102-based cells has better performance than A101-based cells since the results from controlled intermolecular interactions, which the vertical charge transport was improved. However, the poor solubility of A101 devices remains a problem.

In this report, we designed and synthesized D–π–D type HTM (the code name is **PEH-16**), incorporating TIPs-anthracene derivative as a π-conjugation part and dimethoxy-

triphenylamine as a donor part for PSCs. Anthracene moieties are widely used in molecular semiconductors owing to their planarity, which facilitates charge transport by enhancing π-π stacking. Moreover, TIPs (triisopropylsilylacetylene) moiety is used to enhance their solubility and maintain charge transport. The new compound was characterized by conventional spectroscopic/analytical/performance of PSC. PSCs using triplecation-perovskite [22] $Cs_{0.1}(FAPbI_3)_{0.76}(MAPbBr_3)_{0.14}$ and **PEH-16** as HTM exhibited excellent PCE of 17.12% under full son illumination. Also, the stability of **PEH-16** device is quite good compared to the Spiro_OMeTAD device.

2. Materials and Methods

General Methods. All reactions were carried out under nitrogen. All reagents were purchased from Sigma-Aldrich and TCI. ^1H and ^{13}C nuclear magnetic resonance (NMR) spectra were recorded in NMR solvent using a Bruker Fourier 300 MHz spectrometer operated at 300.1 and 75.4 MHz, respectively. The ^1H and ^{13}C NMR chemical shifts were referenced relative to $CDCl_3$ (7.26 ppm for ^1H NMR and 77.16 ppm for ^{13}C NMR). Mass spectra were recorded on a JEOL JMS-SX102A instrument. The absorption and photoluminescence spectra were measured on a Perkin-Elmer Lambda 950S UV/VIS/NIR spectrometer and a Perkin LS-55 fluorescence spectrometer, respectively.

Electrochemical characterization. Cyclic voltammetry was carried out with a IVIUM Compactstat. A three electrodes system were used and consisted of glassy carbon as working electrode, platinum (wire, diam. 1.0 mm, 99.9% trace metals basis by Sigma-Aldrich, St. Louis, MO, USA) as counter and Ag/Ag+ (0.01M $AgNO_3$) reference electrodes were used with and without ferrocene (Fc/Fc+ as an external reference). Redox potential of HTM were measured in CH_2Cl_2 with 0.1 M $(n\text{-}C_4H_9)_4NPF_6$ as 100 mV s^{-1} of a scan rate.

Synthesis. Target compound of **PEH-16**. In degassed water (20 mL) and dry THF (40 mL), a mixture of Compound **1** (0.7 g, 1 mmol), Compound **2** (1.3 g, 3 mmol), $Pd(PPh_3)_4$ (0.12 g, 0.1 mmol), K_2CO_3 (7.4 g, 5 mmol) were refluxed for 36 h under a nitrogen atmosphere. After cooling to RT, the solution was extract with ether and remove residual water with $MgSO_4$. The solvent was remove and the product was purified by column chromatography (DCM:Hx = 1:1). MS: m/z 1144 [M+]. ^1H NMR (CDCl3): δ 8.82 (d, 2H, 4J = 1.2 Hz), 8.61 (d, 2H, 3J = 9 Hz), 7.87 (dd, 2H, 3J = 9 Hz), 7.65 (d, 4H, 3J = 9 Hz), 7.15 (m, 8H), 7.03 (d, 4H, 3J = 8.7 Hz), 6.86 (m, 8H), 3.82 (s, 12H). 1.30 (s, 42H). $^{13}C\{1H\}$ NMR (CDCl3): δ 156.06, 148.60, 140.95, 138.46, 132.88, 132.46, 131.81, 127.92, 127.78, 126.78, 126.59, 123.6, 120.87, 118.25, 114.84, 104.92, 103.73, 55.65, 19.1, 11.67. Anal. Calc. for C76H84N2O4Si2: C, 79.67; H, 7.40; N, 2.44; O, 5.60; Si, 4.92.

Fabrications. FTO glass (Nippon Sheet) was washed by sonicating in a 2% Hellmanex solution, water, acetone, and ethanol. A TiO_2 blocking layer was deposited to the substrate around 30 nm using the spray pyrolysis method at 450 °C from titanium precursor (TAA) by Sigma-Aldrich in isopropanol. We prepared a bi-Mesoporous layer. TiO_2 mesoporous layers were prepared spin coating and sintering at 500 °C for 30 min. Subsequently, SnO_2 was deposited by spin coating using 0.1 M $SnCl_4$ in H_2O. We carried this out sintered at 190 °C for 1 h. The perovskite solution, $Cs_{0.1}(FAPbI_3)_{0.76}(MAPbBr_3)_{0.14}$, was prepared in mixture anhydrous solvent follow according to the literature [23]. Using this solution, spin-coating is performed at 2000 rpm for 12 s and continuously at 5000 rpm for 30 s, leaving 15 s and dropping triflourotoluene (110 μL). This film is immediately annealed at 100 °C for 1 h. The HTM solutions prepared by 20, 40 mM, and Spiro_OMeTAD prepared by 70 mM in chlorobenzene with additives (TBP, Li-TFSI, FK-209) according to the literature [22]. These solutions were spin-coated by 4000 rpm for 25 s. Finally, a device was made by depositing 70 nm Au through a vacuum deposition method.

Solar cell characterization. We measured and obtained current-voltage curves in air condition from a solar simulator of the Newport company connected to a potential state (keithley). To match the light intensity, KG5 filtered Si diode verified by NREL was used. The active area was corrected using a 0.16 cm^2 of metal mask. The IPCE spectra were measured by IQE 200B equipment. We conducted long-term stability tests using unsealed

device with PEH-16 and Spiro_OMeTAD which were stored in dark conditions with a humidity of approximately 20%.

3. Results

The synthesis method of the new HTM is detailed in Scheme 1. All reactions were carried out in a nitrogen atmosphere and compound **1** was prepared according to the literature [24]. The prepared side donor unit as compound **2** was connected to the conjugated linkers by Pd-catalyzed Suzuki coupling reaction with leading to the final product. The final products, **PEH-16**, was verified by NMR spectroscopy. **PEH-16** dissolves well in common solvents such as methylene chloride, chloroform, chlorobenzene, and THF.

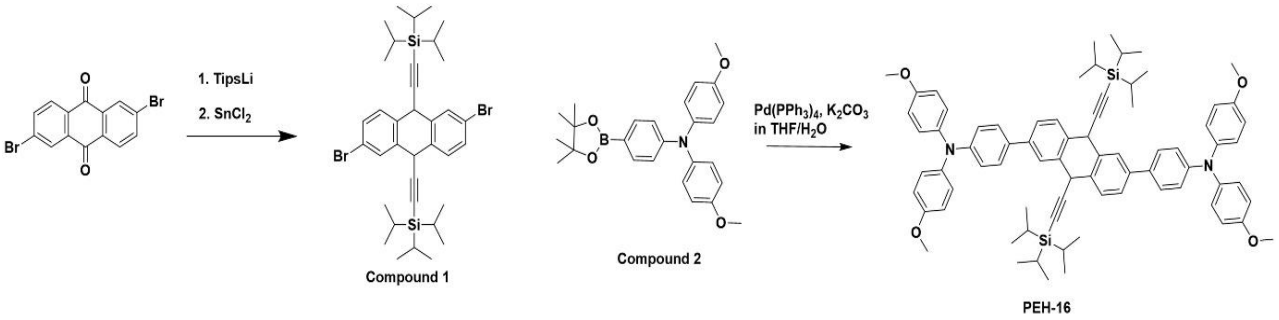

Scheme 1. Synthesis of the new HTM of **PEH-16**.

The UV-vis absorption and photoluminescence spectroscopy of **PEH-16** in THF solution are described in Figure 1a and Table S1. **PEH-16** displayed an absorption maximum at 380, 428, and 505 nm, which is converted to π–π* transition of the conjugated system by light. The optical band gab ($E_{0\text{-}0}$) of **PEH-16** is calculated at the intersection of absorption and emission spectra. In Figure S1, we measured thermogravimetric analysis (TGA) to determine the thermal property of **PEH-16**. Thermogravimetry analysis (TGA) showed that **PEH-16** start to decompose at temperature higher than 350 °C and they encounter 30% weight loss after 400 °C. This demonstrated a superior thermal stability of **PEH-16** incorporated with TIPs-anthracene-linked dimethoxytriphenylamine as a hole transporting material for PSCs.

The electrochemical properties of **PEH-16** were studied using cyclic voltammetry (CV) in Figure 1b and Table S1. **PEH-16** show reversible redox processes in the low potential region at 0.19 V, indicating that the two electrons are removed successively from TPA donor units. The HOMO level of **PEH-16** was calculated using CV with ferrocene as reference. Since the calculated HOMO level is −5.24 eV, which is higher than the valence band (−5.65 eV) of perovskite, the new HTM can have an efficient hole transport capability. According to $E_{LUMO} = E_{HOMO} - E_{0\text{-}0}$, the LUMO level of **PEH-16** was calculated to be −2.91 eV, which plays an important role of HTM in operating for PSCs. When electrons are excited in the perovskite, not only does it prevent the counter electrode electrons from flowing, but it also ensures that they flow naturally to the perovskite layer when electrons of the HTMs are excited in Figure 1c.

In the seen Figure 2a, the photoluminescene (PL) spectra exhibited the perovskite film with and without HTMs. As a typical result, the device with HTM shows dramatic quenching with respect to the pristine perovskite. Reduced of PL intensity is attributable to the effective hole transport occurring at interfacial of the perovskite and HTM. The new HTM shows an effective PL quenching than Spiro_OMeTAD. This reduction in perovskite PL can result in efficient hole transport from perovskite to **PEH-16**. However, since **PEH-16** emission partially overlap with the perovskite, these numbers do not pretend to be quantitative but still indicate that a lot of quenching occurs.

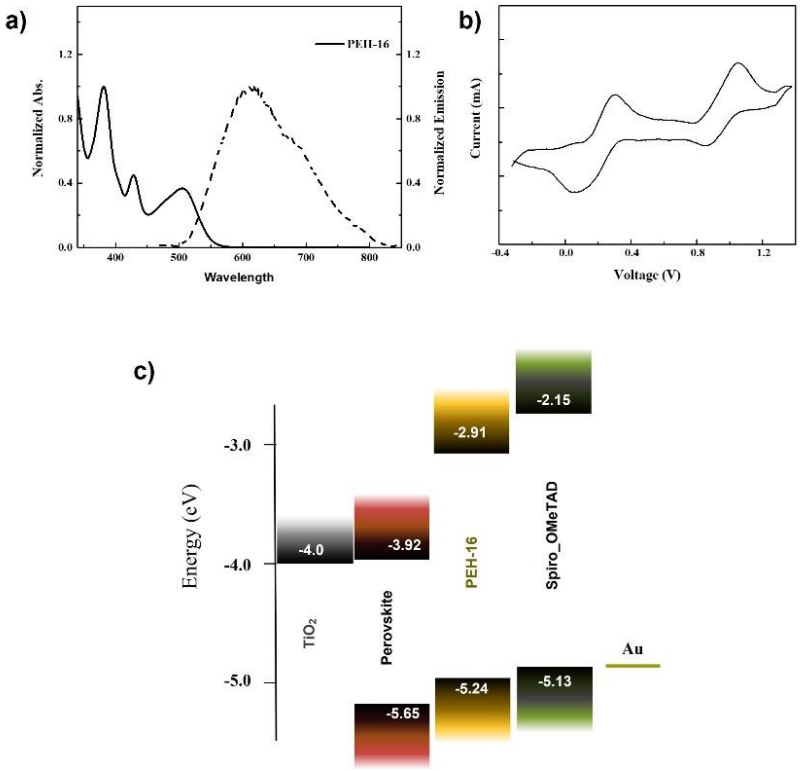

Figure 1. (**a**) Absorption (black solid line) and photoluminescence (black dashed line) spectrum of **PEH-16** in THF. (**b**) Cyclic voltammogram of **PEH-16** in DCM with 0.1 M tetrabutylammonium hexafluorophosphate. (**c**) Energy level diagram of each material in perovskite solar cell.

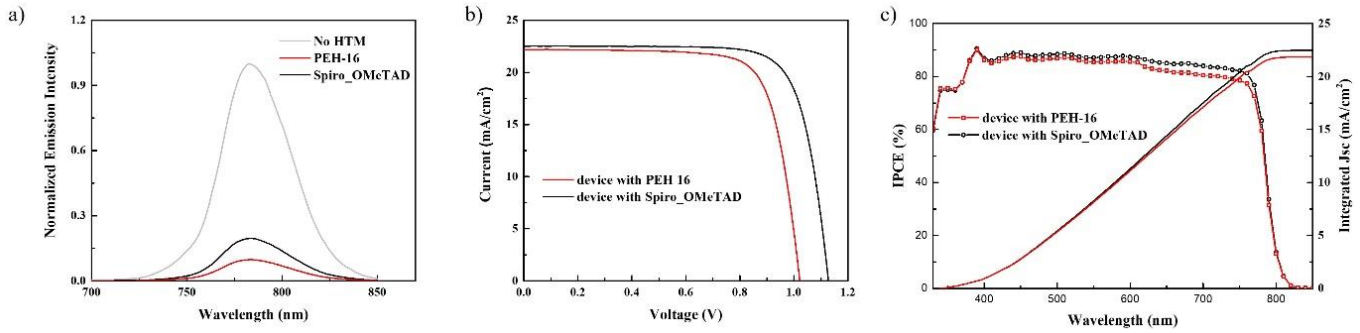

Figure 2. (**a**) Steady state PL spectra of pristine perovskite and perovskite/HTM bilayer under excitation at 530 nm. (**b**) Current-voltage curves of the best performing device using **PEH-16** and Spiro_OMeTaD. (**c**) IPCE spectra of the device using HTM and integrated Jsc from the IPCE curves.

To investigate the PEC of **PEH-16** and Spiro-OMeTAD for PSCs, the device configuration of FTO/compact and mesoporous $TiO_2/SnO_2/Cs_{0.1}(FAPbI_3)_{0.76}(MAPbBr_3)_{0.14}$/HTM/Au was fabricated by an anti-solvent method [22,25]. A detailed procedure is shown in the ESI.

A device was fabricated using different concentrations, and the optimal efficiency of the device was reported using a concentration having a high efficiency among them. Then, current-voltage (J-V) curves of device with **PEH-16** and Spiro_OMeTAD are provided in Figure 2b and their PV parameters are summarized in Table 1. The best performing device with **PEH-16** exhibited an PCE of 17.12% under standard AM 1.5 illumination (100 mW cm^{-2}) (open-circuit voltage (Voc) of 1.022 V, a short-circuit current (JSC) of 22.19 mA cm^2, and a fill factor (FF) of 0.755, respectively). The performing device with Spiro_OMeTAD showed over 19% efficiency slightly higher Voc and Jsc under the same conditions. In order to confirmed the change of Jsc based on different HTMs, we conducted

incident photon-to-current conversion efficiency (IPCE) spectrum in Figure 2c. The integrated Jsc values from the IPCE spectra were 21.9, and 22.5 for **PEH-16** and Spiro_OMeTAD, respectively, which is consistent with the value of short-circuit current in Figure 2b. As seen in Figure S2 and Table 1, both cells of hysteresis between reverse and forward were almost invisible. Due to slightly lower Voc and ff, we obtained low performance in the forward scan.

Table 1. Photovoltaic performance of the **PEH-16** and Spiro_OMeTAD devices under one sun illumination.

		Voc (V)	Jsc (mA cm^{-2})	ff	Efficiency (%)
PEH-16	Best	1.022	22.19	0.755	17.12
	Reverse scan	1.036	22.46	0.710	16.51
	Forward scan	1.020	22.46	0.690	15.81
Spiro_OMeTAD	Best	1.127	22.51	0.767	19.46
	Reverse scan	1.117	22.58	0.750	18.90
	Forward scan	1.105	22.59	0.735	18.34

The stability of the PSCs is one of the main factors, and we performed a stability test of the device with **PEH-16**. Spiro_OMeTAD was also implemented for comparing. The devices were kept without encapsulation in ambient condition (around 20% relative humidity in dark). As seen in Figure S3 and Table S2, the stability of both devices is very interesting and shows an increased efficiency compared with the initial efficiency for 1200 h. In addition, when the highest efficiency is seen as a standard, the **PEH-16** and Spiro_OMeTAD based on the device exhibit a reduction 2% and 3%, respectively. We confirmed improvement in the stability of devices based on **PEH-16**.

In summary, we have designed and synthesized simple hole transporting materials that incorporated Tips-anthracene as a π–conjugation part with good solubility by a facile synthesis process. The novel HTM has an appropriate energy level and efficient hole transport occurring between the perovskite and HTM interface. The optimized device with **PEH-16** achieved a PCE of 17.12%. Moreover, we demonstrated significantly improved long-term stability of device with **PEH-16** comparable to the device with Spiro_OMeTAD. Work related to the design and development of a new anthracene-based HTM which is dopant-free and has a higher stability is currently in progress.

Supplementary Materials: The following are available online at https://www.mdpi.com/article/10.3390/pr9122249/s1. Figures S1–S5, Tables S1 and S2. Table S1. Optical and electrochemical data for PEH-16. Figure S1. Thermogravimetry analysis (TGA) of PEH-16. Figure S2. Hysteresis of device with PEH-16 and Spiro_OMeTAD. Figure S3. Stability test for device base on PEH-16 and Spiro_OMeTAD during 1200 h. Table S2. A summary of stability data. Figure S4. 1H NMR of PEH-16. Figure S5. ^{13}C NMR of PEH-16.

Funding: The author acknowledges the financial support by a 2020 research Grant from Sangmyung University.

Institutional Review Board Statement: Not applicable.

Informed Consent Statement: Not applicable.

Data Availability Statement: Not applicable.

Acknowledgments: I thank Wonsik Han, Seoul Women's University for providing NMR.

Conflicts of Interest: The authors declare no conflict of interest.

References

1. Xing, G.; Mathews, N.; Sun, S.; Lim, S.S.; Lam, Y.M.; Graẗzel, M.; Mhaisalkar, S.; Sum, T.C. Long-Range Balanced Electron- and Hole-Transport Lengths in Organic-Inorganic CH3NH3PbI3. *Science* **2013**, *342*, 344–347. [CrossRef]
2. de Wolf, S.; Holovsky, J.; Moon, S.J.; Löper, P.; Niesen, B.; Ledinsky, M.; Haug, F.J.; Yum, J.H.; Ballif, C. Organometallic Halide Perovskites: Sharp Optical Absorption Edgeand Its Relation to Photovoltaic Performance. *J. Phys. Chem. Lett.* **2014**, *5*, 1035–1039. [CrossRef]
3. Stranks, S.D.; Eperon, G.E.; Grancini, G.; Menelaou, C.; Alcocer, M.J.P.; Leijtens, T.; Herz, L.M.; Petrozza, A.; Snaith, H.J. Electron-Hole Diffusion Lengths Exceeding 1 Micrometer in an Organometal Trihalide Perovskite Absorber. *Science* **2013**, *342*, 341–344. [CrossRef]
4. Shi, D.; Adinolfi, V.; Comin, R.; Yuan, M.; Alarousu, E.; Buin, A.; Chen, Y.; Hoogland, S.; Rothenberger, A.; Katsiev, K.; et al. Low trap-state density and long carrier diffusion in organolead trihalide perovskite single crystals. *Science* **2015**, *347*, 519–522. [CrossRef]
5. NREL Research Cell Record Efficiency Chart. Available online: https://www.nrel.gov/pv/assets/pdfs/best-research-cell-efficiencies-rev210726.pdf (accessed on 30 October 2021).
6. Chen, Y.; Xu, X.; Cai, N.; Qian, S.; Luo, R.; Huo, Y.; Tsang, S.-W. Rational Design of Dopant-Free Coplanar D-π-D Hole-Transporting Materials for High-Performance Perovskite Solar Cells with Fill Factor Exceeding 80%. *Adv. Energy Mater.* **2019**, *9*, 1901268. [CrossRef]
7. Vegiraju, S.; Ke, W.; Priyanka, P.; Ni, J.-S.; Wu, Y.-C.; Spanopoulos, I.; Yau, S.L.; Marks, T.J.; Chen, M.-C.; Kanatzidis, M.G. Benzodithiophene Hole-Transporting Materials for Efficient Tin-Based Perovskite Solar Cells. *Adv. Funct. Mater.* **2019**, *29*, 1905393. [CrossRef]
8. Zimmermann, I.; Aghazada, S.; Nazeeruddin, M.K. Lead and HTM Free Stable Two-Dimensional Tin Perovskites with Suitable Band Gap for Solar Cell Applications. *Angew. Chem. Int. Ed.* **2019**, *58*, 1072–1076. [CrossRef]
9. Ke, W.; Priyanka, P.; Vegiraju, S.; Stoumpos, C.C.; Spanopoulos, I.; Soe, C.M.M.; Marks, T.J.; Chen, M.-C.; Kanatzidis, M.G. Dopant-Free Tetrakis-Triphenylamine Hole Transporting Material for Efficient Tin-Based Perovskite Solar Cells. *J. Am. Chem. Soc.* **2018**, *140*, 388–393. [CrossRef]
10. Liu, X.; Zhang, F.; Liu, Z.; Xiao, Y.; Wang, S.; Li, X. Dopant-free and low-cost molecular "bee" hole-transporting materials for efficient and stable perovskite solar cells. *J. Mater. Chem. C* **2017**, *5*, 11429–11435. [CrossRef]
11. Li, H.; Fu, K.; Hagfeldt, A.; Grätzel, M.; Mhaisalkar, S.G.; Grimsdale, A.C. A Simple 3,4-Ethylenedioxythiophene Based Hole-Transporting Material for Perovskite Solar Cells. *Angew. Chem. Int. Ed.* **2014**, *53*, 4085–4088. [CrossRef]
12. Abate, A.; Paek, S.; Giordano, F.; Correa-Baena, J.P.; Saliba, M.; Gao, P.; Matsui, T.; Ko, J.; Zakeeruddin, S.M.; Dahmen, K.H.; et al. Silolothiophene-linked triphenylamines as stable hole transporting materials for high efficiency perovskite solar cells. *Energy Environ. Sci.* **2015**, *8*, 2946–2953. [CrossRef]
13. Rakstys, K.; Paek, S.; Drevilkauskaite, A.; Kanda, H.; Daskeviciute, S.; Shibayama, N.; Daskeviciene, M.; Gruodis, A.; Kamarauskas, E.; Jankauskas, V.; et al. Carbazole-Terminated Isomeric Hole-Transporting Materials for Perovskite Solar Cells. *ACS Appl. Mater. Interfaces* **2020**, *12*, 19710–19717. [CrossRef] [PubMed]
14. Luizys, P.; Xia, J.; Daskeviciene, M.; Kantminiene, K.; Kasparavicius, E.; Kanda, H.; Zhang, Y.; Jankauskas, V.; Rakstys, K.; Getautis, V.; et al. Branched Methoxydiphenylamine-Substituted Carbazole Derivatives for Efficient Perovskite Solar Cells: Bigger Is Not Always Better. *Chem. Mater.* **2021**, *33*, 7017–7027. [CrossRef] [PubMed]
15. Saliba, M.; Orlandi, S.; Matsui, T.; Aghazada, S.; Cavazzini, M.; Correa-baena, J.P.; Gao, P.; Scopelliti, R.; Mosconi, E.; Dahmen, K.H.; et al. A molecularly engineered hole-transporting material for efficient perovskite solar cells. *Nat. Energy* **2016**, *1*, 15017. [CrossRef]
16. Nawar, A.M.; Yahia, I.S. Fabrication and characterization of anthracene thin films for wide-scale organic optoelectronic applications based on linear/nonlinear analyzed optical dispersion parameters. *Opt. Mater.* **2017**, *70*, 1–10. [CrossRef]
17. Yutaka, M.; Hiroshi, O.; Yasuhiro, K.; Jeon, H.W.; Yun, Y.; Takeshi, M.; Motoki, Y.; Toshiaki, I. Anthracene-Based Organic Small-Molecule Electron-InjectingMaterial for Inverted Organic Light-Emitting Diodes. *ACS Appl. Mater. Interfaces* **2018**, *10*, 11810–11817.
18. Inoue, Y.; Tokito, S. Organic thin-film transistors based on anthracene oligomers. *J. Appl. Phys.* **2004**, *95*, 5795. [CrossRef]
19. Choi, H.; Ko, H.M.; Cho, N.; Song, K.; Lee, J.K.; Ko, J. Electron-Rich Anthracene Semiconductors Containing Triarylamine for Solution-Processed Small-Molecule Organic Solar Cells. *Chemsuschem* **2012**, *5*, 2045–2052. [CrossRef]
20. Kayani, K.Q.; Yaqoob, U.; Jabeen, S.; Iqbal, S.; Yaseen, M.; Khalid, M.; Akhter, M.S.; Iqbal, J. Tris-isopropyl-sily-ethynyl anthracene based small molecules for organic solar cells with efficient photovoltaic parameters. *Comput. Theor. Chem.* **2021**, *1202*, 113305. [CrossRef]
21. Liu, X.; Kong, F.; Ghadari, R.; Jin, S.; Yu, T.; Chen, W.; Liu, G.; Tan, Z.; Chena, J.; Dai, S. Anthracene–arylamine hole transporting materials for perovskite solar cells. *Chem. Commun.* **2017**, *53*, 9558–9561. [CrossRef]
22. Saliba, M.; Matsui, T.; Seo, J.-Y.; Domanski, K.; Correa-Baena, J.-P.; Nazeeruddin, M.K.; Zakeeruddin, S.M.; Tress, W.; Abate, A.; Hagfeldtd, A.; et al. Cesium-containing triple cation perovskite solar cells: Improved stability, reproducibility and high efficiency. *Energy Environ. Sci.* **2016**, *9*, 1989–1997. [CrossRef] [PubMed]
23. Cho, K.T.; Grancini, G.; Lee, Y.; Oveisi, E.; Ryu, J.; Almora, O.; Tschumi, M.; Schouwink, P.A.; Seo, G.; Heo, S.; et al. Selective growth of layered perovskites for stable and efficient photovoltaics. *Energy Environ. Sci.* **2018**, *11*, 952–959. [CrossRef]

24. Park, J.-H.; Chung, D.S.; Park, J.-W.; Ahn, T.; Kong, H.; Jung, Y.K.; Lee, J.; Yi, M.H.; Park, C.E.; Kwon, S.-K.; et al. Soluble and Easily Crystallized Anthracene Derivatives: Precursors of Solution-Processable Semiconducting Molecules. *Org. Lett.* **2007**, *9*, 2573–2576. [CrossRef] [PubMed]
25. Jeon, N.J.; Noh, J.H.; Kim, Y.C.; Yang, W.S.; Ryu, S.; Seok, S.I. Solvent engineering for high-performance inorganic–organic hybrid perovskite solar cells. *Nat. Mater.* **2014**, *13*, 897–903. [CrossRef] [PubMed]